CLM-P 393

THE THERMAL CONTAINMENT OF REACTOR CORE MATERIAL AFTER SHUTDOWN

R S Peckover

(Paper presented at the ANS Fast Reactor Safety Meeting, Los Angeles, April 1974)

ABSTRACT

A temperature excursion arising through some hypothetical blockage of the cooling system in a liquid cooled reactor system could lead to the melt-out of the core or part of the core. One way of containing the core débris may be to allow it to fall into suitably designed core catchers placed below the core subassemblies. An alternative approach would be to allow the core material to settle on the bottom of the reactor pot which is cooled from below by forced convection. A third possibility is to allow the core to fall into a subterranean cavity built especially for the purpose.

Any calculations of the heat fluxes depend on the transport processes involved. Often only thermal conduction is assumed and a number of detailed calculations have been made on this basis. Thermal convection within the heat-producing core débris modifies the heat transfer coefficients from the débris and the maximum temperatures within it. In this paper an indication is given of the extent to which more detailed calculation of internally heated thermal convection may alter current thinking on reactor safety.

UKAEA Research Group
Culham Laboratory
Abingdon, Berks.

March 1974

dg

INTRODUCTION

This paper is concerned with thermal containment after shutdown. A hypothetical reactor incident is postulated in which the cooling system is at least temporarily blocked, and a temperature excursion arises in the core. A subassembly or a substantial fraction of the core melts, and the reactor is shut down. How can the overheated core material be cooled while being confined to a safe place? Different strategies may be required depending upon what sequence of events is envisioned.

I want to consider three broad classes of possible core catcher incidents:

(1) A fraction of the core melts, due to a failure of the cooling system, but this failure is only local. Coolant remains present. The molten core material falls onto core catchers lying inside the reactor vessel, and remains there to be cooled. If most of the coolant is expelled, but subsequently the emergency core cooling system injects coolant then the same general scenario is appropriate.

(2) A fraction of the core melts and falls onto the bottom of the reactor vessel. Coolant remains in the reactor vessel, and, provided the integrity of the reactor vessel is maintained then the core material is cooled in situ.

(3) A fraction of the core melts and falls through into a pit provided for the purpose. No coolant is present and the core material cools by radiation upwards and conduction downwards through the structure supporting it. If the core material falls onto the bottom of the reactor vessel and coolant is absent then the configuration is conceptually similar.

In class 1, internal core catchers are involved; in class 3, external core catchers are central. Class 2, involving the bottom of the reactor pot, is a sort of hybrid which can be viewed partly as internal and partly as external. All work on core catchers and the thermal containment after shutdown has been concerned with these three broad possibilities. Figure 1 illustrates some possible core catcher configurations, in stylized fashion. For internal core catchers it may well be that a number of catchers in a suitable array will be required. For the present, only one isolated internal catcher is considered.

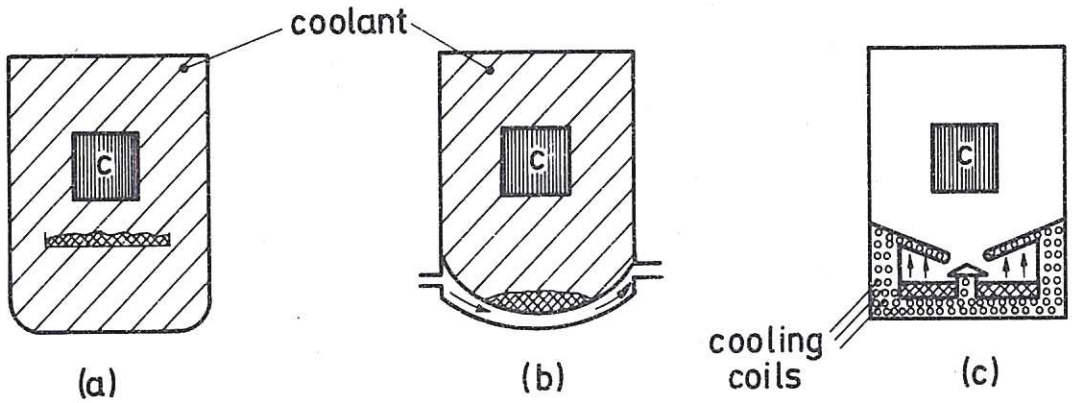

Figure 1. Configurations after shutdown C = normal location of core

(a) core débris on internal catcher: coolant present

(b) core débris on bottom of reactor pot: coolant present. Additional cooling provided below the reactor pot.

(c) core débris in cooling trap surrounded by cooling coils. No coolant above - radiational heat transfer upwards (after Barleon, Dalle Donne, and Dorner [1972]).

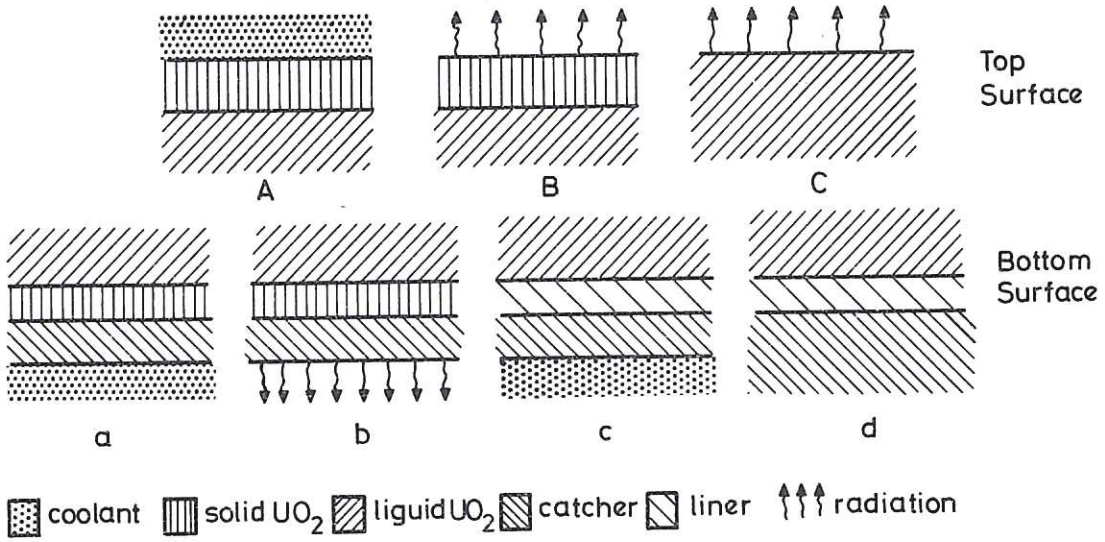

Figure 2. Classification of boundary configurations above and below a layer of molten UO_2 in a core catcher after shutdown (see also Table 1).

Core Catcher Configurations

The molten material may fall down as large heterogeneous lumps of fuel, fuel pin casing, subassembly support, and diagrid. Or, if a mild FCI has occurred (Buchanan (1973), Buchanan and Dullforce (1973), Board et al (1972)), it may be in the form of dispersed particulate débris. The cooling of the dispersed débris if the coolant is present, gives no problems except where the débris forms into a bed of particulate material. It seems (Peckover (1973), Baker and Gabor (1972)) that either the débris will be cooled satisfactorily, or it will overheat and melt to form a layer from which the coolant has been expelled, for which a molten layer analysis is appropriate.

If one assumes that a lump occurs (or lumps), then at its greatest depth one may examine the structure of a vertical section, and can distinguish a number of different cases. I am going to use a horizontal 'layer cake' model, not because such will necessarily occur, but because this provides the simplest model. More complex configurations can be considered to be modifications to the layer of configuration.

What can be said if conduction were the only transport mechanism within the core débris? Consider a layer of UO_2 producing fission product heat of 30 MW/m^3, then if the maximum temperature in the layer is constrained to be the boiling temperature of UO_2, then the thickness of the layer cannot exceed $\simeq$ 4 cm. This heating rate (H), being 2% of full FR power, corresponds to 30 minutes after shutdown (Teague 1965) and assumes efficient cooling above and below the core débris. Crudely, the layer depth $\propto H^{-\frac{1}{2}}$, so that at 4% of full FR power ($\simeq$ 2 minutes after shutdown), the layer depth would be $\simeq 2\frac{1}{2}$ cm and at 1% of full FR power ($\simeq$ 5 hours after shutdown) the power layer depth of a stable conductive layer rises to $\simeq$ 6 cm. The decay heat falls rapidly with time so that it is only 6% of full power only a few seconds after shutdown (Teague 1965). It seems reasonable to assume that the strong diagrid will obstruct the passage downwards of the core débris at least for that period of time. The presence of fuel can, and other essentially non-radiactive materials may increase the depth of caught material by another factor of two (Peckover 1973). Similar statements though with different numerical values can be made about water reactors (Ergen et al (1967)).

Clearly if conduction were the only transport mechanism in the UO_2 then, unless the core débris flows into a shallow layer covering almost the whole cross-sectional area of the reactor pot, the maximum temperature of the material of the whole core would exceed its boiling point whenever core débris reached

the catchers in significant quantities before something like two minutes had elapsed after shutdown. Equally clearly, the meltdown of a single subassembly to produce a molten pool of fuel and fuel can débris could be cooled in an internal core catcher by conduction alone, without invoking the other heat transport mechanisms which could be present. The successful cooling of a partial meltdown using an internal core catcher would avoid damage to the bottom of the reactor pot; if this resulted in the reactor returning earlier to service, considerable economic benefits could accrue.

However, molten material can convect and under suitable thermal conditions provides an effective mechanism for heat transport. What effect will this have on the amount of material which can be accomodated in the steady state of the core catcher? Figure 2 consists of a classification of the different top and bottom boundary conditions which apply to a layer of molten UO_2 . The list in Table 1 illustrates how the top and bottom configurations combine together for any particular core catcher whether internal, external, or the reactor pot bottom itself. The complicating effect of additional (steel) débris without additional radioactive heat sources has been omitted from this classification and will be discussed later in this paper.

The point of this analysis is that the core débris must be cooled mainly in one of these configurations if it is successfully cooled at all (apart from particulate cooling which either is successful or reduces to one of the above cases). Of course the problem of core cooling is a time dependent one and the very early stages after shutdown can be important. Epstein (1972) has carried out a time dependent analysis for a multi-layer 'cake' in which only conduction occurs. However as the work of Teague (1965) has shown, the time scales for the decay of the radioactive heating are soon long compared with the conductive (and a fortiori the convective) time scales so that we may profitably consider model problems in which the volumetric heating rate is a specified function of position.

Convective Layer Models

A number of different configurations for core catchers have been presented in Figure 2 and Table 1. However if we concentrate our attention on the molten layer only, it has a much smaller number of possible boundary conditions. At the top of the molten layer, either a solid crust exists which must have an interface temperature at the melting point of UO_2 (T melt $\simeq$ 3100K), or the molten layer radiates directly in a cavity (the reactor vessel) which may contain low density gas, so that a radiation boundary condition applies. At the lower surface of the molten layer either a solid crust of heat producing UO_2

TABLE 1.

Typical core catcher configurations classified according to boundary conditions on the molten layer of débris (see Fig 2)

Aa	Internal catcher or bottom of reactor pot, with external cooling
Ab	Bottom of reactor pot - failure of external cooling
Ac	Internal catcher or bottom of reactor pot with external cooling and a liner of low thermal conductivity eg. depleted UO_2 or carbon
Ad	External catcher with coolant above
Ba	Bottom of reactor pot with external cooling, but no internal cooling
Bb	Internal catcher - no coolant around it
Bc	Lined internal catcher or lined bottom of reactor pot with external cooling but no internal cooling
Bd	External catcher with no coolant above
Ca, Cb, Cc, Cd	As for cases B but no solid skin forms on the top of the molten UO_2 which radiates from its liquid upper surface into the pot or external catcher cavity

exists below it so far that the interface temperature is T_{melt} , or a passive liner with low heat transmission is present which may be approximated by a thermal insulator. Thus there are only four convective layer models to consider, and these are shown schematically in Figure 3.

I Kulacki-Goldstein Model

Both upper and lower surfaces of the molten layer are at the same fixed temperature. The first laboratory experiments on the problem were carried out by Kulacki and Goldstein (Kulacki (1971), Kulacki and Goldstein (1972)).

II Tritton-Zarraga Model

The upper surface is held at a fixed temperature; the lower surface is a thermal insulator:

$$\frac{\partial T}{\partial z} = 0 \quad (z \text{ is the vertical co-ordinate})$$

The first laboratory experiments on this model problem, which has obvious geophysical relevance to the earth's mantle, were carried out in Newcastle as early as ten years ago (Tritton and Zarraga (1967)).

III Quasi-Whitehead-Chen Model

The lower surface is held at a fixed temperature, the upper surface is in radiative equilibrium, and satisfies the radiation boundary condition. Whitehead and Chen (1970) have carried out a closely related experiment.

IV The Planetary Skin Model

The lower surface of the molten layer is a thermal insulator, the upper surface satisfies the radiation boundary condition. This has close similarities with some models of convection in the atmosphere of Venus.

In the following sections it is convenient to characterize the Rayleigh number of the fluid layer by R^*, which is the ratio of the Rayleigh number (however it may be defined) to the critical Rayleigh number appropriate for these boundary conditions. Numerical values for the critical Rayleigh numbers are gathered together for reference in the Appendix I.

The Kulacki-Goldstein Model

We consider a horizontal layer of fluid containing a uniform distribution of volumetric heat sources which lies between two flat horizontal isothermal surfaces of the same temperature (the melting temperature of UO_2 for example).

Whenever radiation does not enter a model's formulation, as in this case, then only temperature differences are important, and the 'temperature' origin may be defined for convenience. The layers of solid UO_2 above and below the molten layer mean that $\underline{v} = o$ is the appropriate boundary condition (no slip). Kulacki and Goldstein (1972) have carried out elegant experiments using the Joule heating of aqueous silver nitrate for $R^* \leqslant 675$. More recently Jahn and Reineke (1973) have also carried out a series of experiments using holographic techniques and have extended their results to $R^* \simeq 2.10^4$. Their good agreement for the fraction of heat emerging upwards, μ, and for the reduction of the maximum temperature from what it would have been in the absence of convection (M^{-1}) is shown in Figures 4 and 5. Numerical simulation experiments have been carried out by Jahn and Reineke for non-slippery boundaries where the motion has been restricted to two dimensions. Peckover and Hutchinson (1973a) have performed similar calculations for slippery boundaries. All of these have been for a Prandtl number close to that of water ($\simeq 7 \pm 2$). The Prandtl number of UO_2 is not well determined, but if Tsai and Olander's (1972) values are used for the viscosity, then a value of unity (Chasanov et al (1974)) is appropriate. Peckover and Hutchinson (1974) have extended their numerical simulations to include a variation in Prandtl number, and find that for internally heated fluids there are two regimes: (i) $Pr \gg 1$ and (ii) $Pr \lesssim 1$ as there are for the Bénard problem for certain ranges of R^* (Moore and Weiss (1973)). Figure 6 shows the dependence of Pr. For large Pr the flux ratio tends to the asymptotic value calculated using the shape assumption of Stuart.

From Figure 4, the fraction of the internal heat emerging from the top increases with increasing R^* (ie. with the heating rate). However the absolute magnitude of the heat emerging through the lower surface does not fall, but itself increases slowly. At low R^* ($\lesssim 10$), the convection has fairly steady patterns for slippery boundaries. This can result in long-lived areas developing on the upper and lower boundaries, where the vertical heat flux significantly exceeds the horizontal average. These can put thermal stress on the solid and assist in scalloping the horizontal surfaces. For slippery boundaries in the laboratory experiments and for non-slippery boundaries for $R^* \leqslant 10$ in the numerical simulations, the fluid though composed at any instant of irregular-looking cells is neither truly periodic nor stationary. The essential characteristic of internally heated fluids is a broad slowly rising region punctuated by narrow falling plumes of fluid which has given up its heat in the upper boundary layer. Unlike Bénard convection, there is effectively no lower boundary layer. At high R^* the convection is turbulent, and the temperature in the main body of the fluid is consistent with an upper boundary layer with a mean conductive

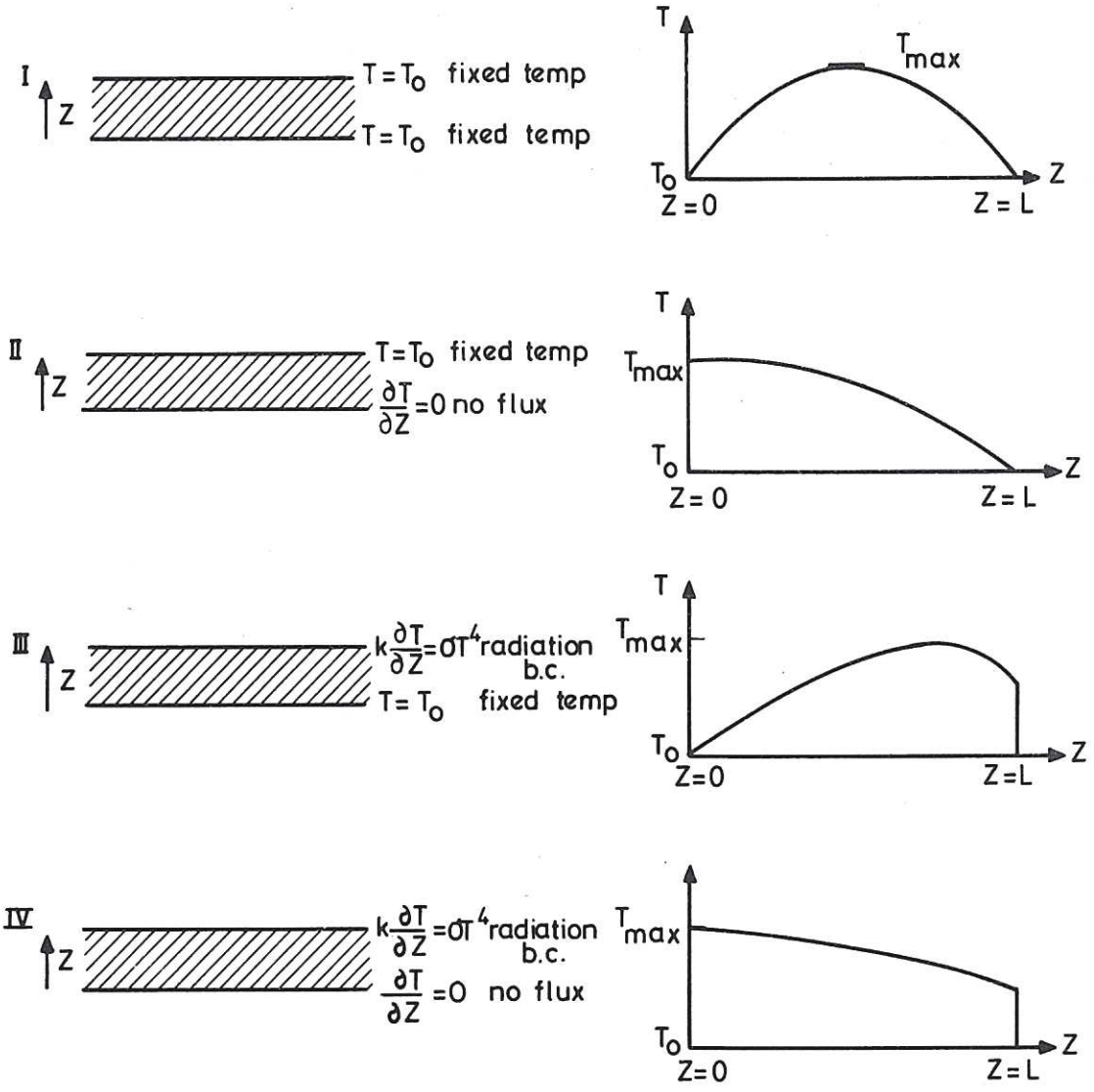

Figure 3. The four cases shown represent the boundary conditions for a molten layer with volumetric heat sources appropriate to core catcher studies. The curved profiles through the layers are the conduction solutions in the absence of convection. I Kulacki-Golstein, II Tritton-Zarraga, III Quasi-Whitehead-Chen, IV Planetary Skin Model.

profile (see figure 7). Catton and Suo-Anttila (1973) have calculated the flux ratio using an expansion technique based on eigenmodes and get good agreement for $R^* \lesssim 10$ for non-slippery boundaries.

The Tritton-Zarraga Model

The experiments of Tritton and Zarraga concentrated on the occurrence of hexagonal cells and seemed to indicate that internally heated convection might have cell size increasing with R^*, rather than decreasing as is the norm for Bénard convection (Brindley (1967)). However Schwiderski and Schwab redid these experiments and showed conclusively (Schwiderski and Schwab (1971), Schwiderski (1972)) that the temperature dependence of the electrical conductivity leads to spatially non-uniform volumetric heating, and that this is likely to cause the hexagons to swell. Roberts (1967) did a mean field analysis which is accurate for low R^* and Thirlby (1970) carried out a numerical simulation for both two and three dimensional convection. The fall in the maximum temperature relative to the conduction maximum is shown in Figure 8. The results of Schwiderski and Schwab for which the heating is known to be non-uniform ($\Delta H \propto \Delta T$) is also shown. More recently McKenzie, Roberts and Weiss (1974) have carried out a series of numerical simulations with the earth's mantle in mind and have obtained results, for two-dimensional flows, for $R^* \lesssim 1600$. A few points from their analysis are included.

The Quasi-Whitehead-Chen Model

The lower surface is at a fixed temperature (the melting temperature) and is a rigid solid boundary. The upper surface is free and is at a higher temperature but less than the maximum within the layer. The upper boundary temperature (which varies horizontally) is the result of a balance between conduction to the surface, and radiation from the surface into (cold) space. Thus a potentially unstable layer overlays a layer which is in itself stable. Such a case has not been examined as yet but Whitehead and Chen (1970) have examined a closely allied case in which the upper boundary is maintained at a temperature exceeding the lower boundary and is rigid rather then free. A convex conductive profile is produced using radiant heating, and is close to parabolic over part of the layer depth. As the temperature of the upper surface is lowered towards that of the bottom surface, so the Whitehead-Chen configuration approximates to the Kulacki-Goldstein problem. The Whitehead-Chen model is basically concerned with a shallow unstable layer over a deep stable layer, whereas the potentially stable and unstable layers are equal in the Kulacki-Goldstein problem. Nevertheless Whitehead and Chen also find narrow falling jets (narrower in fact), but their influence is understandably less.

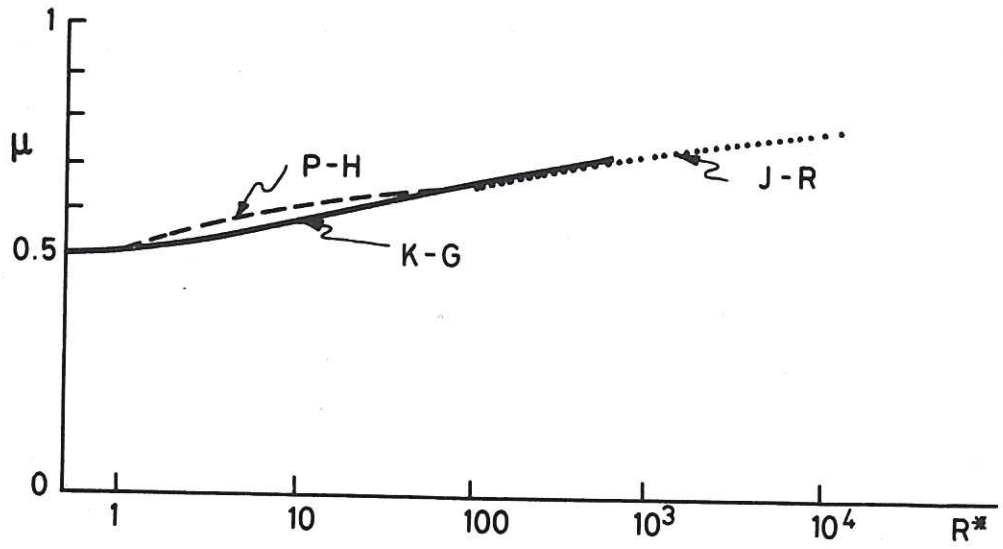

Figure 4. The fraction of upward flux $\mu \equiv (Nu_{up}/[Nu_{up} + Nu_{down}])$ as a function of R^*. J - R ≡ Jahn and Reineke (1973); K - G ≡ Kulacki and Goldstein (1972); P - H ≡ Peckover and Hutchinson (1973a). These are for Pr ∿ 7, for model I.

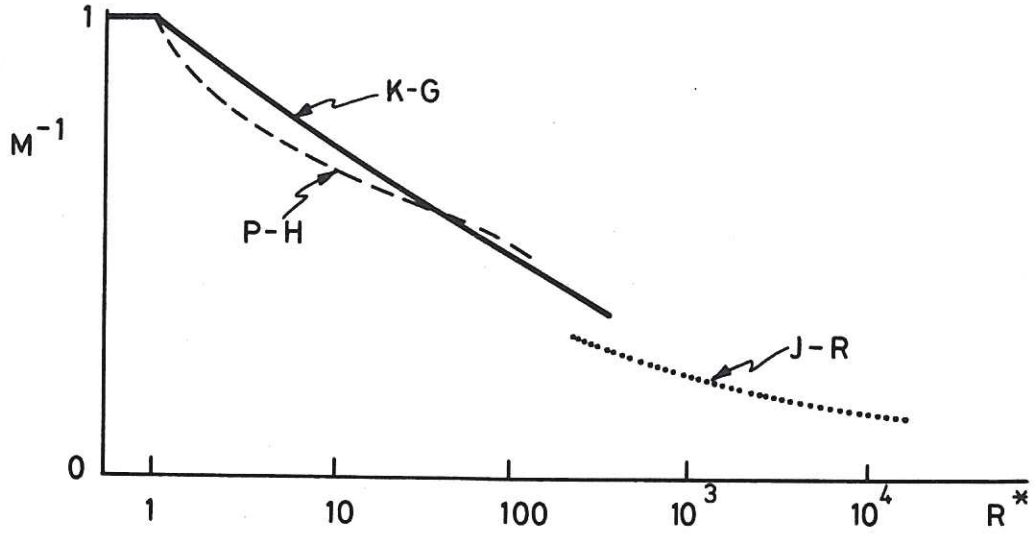

Figure 5. The convective cooling parameter $M \equiv (T^* - T_o/T_{max} - T_o)$ as a function of R^* for model I. See figure 4 for legend.

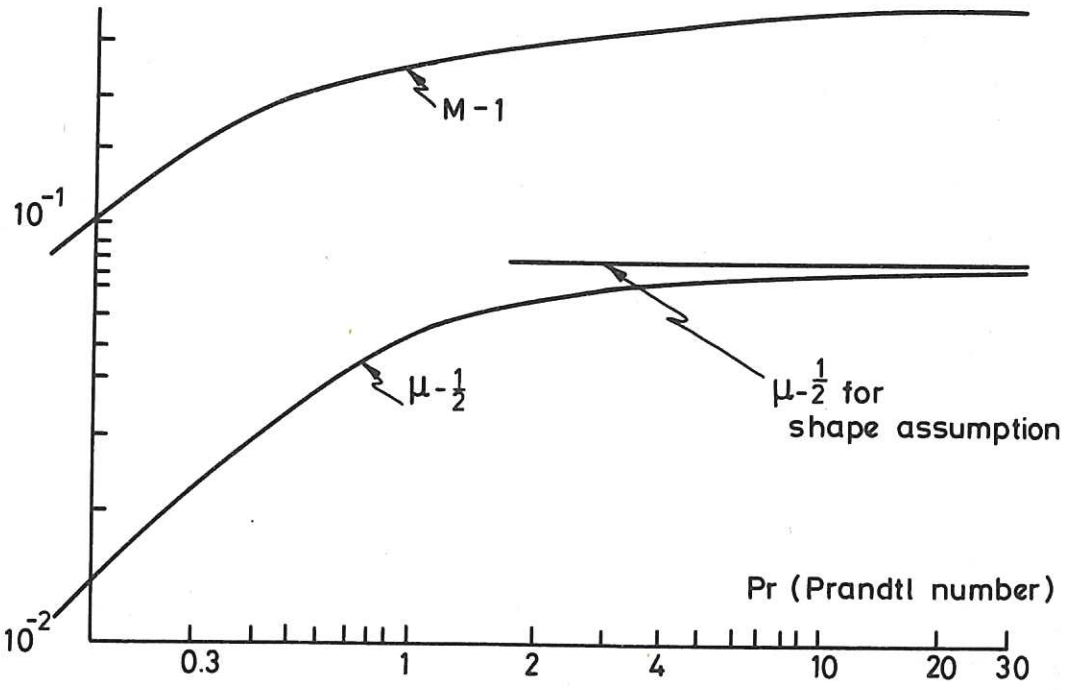

Figure 6. The convective cooling parameter M and the upward flux excess $(\mu - \frac{1}{2})$ as functions of Pr for $R^* = 3$ for case I.

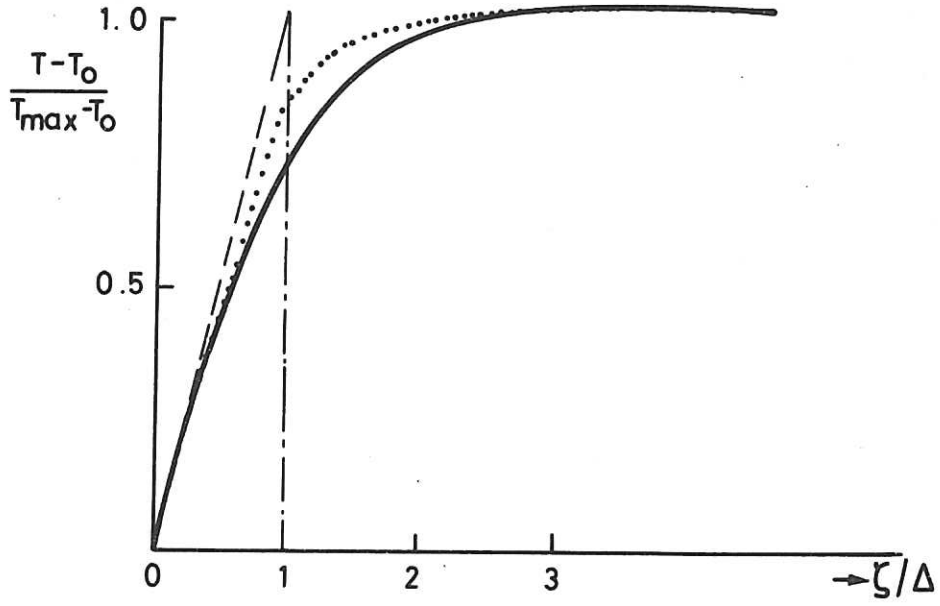

Figure 7. Normalized temperature profile near the upper surface for turbulent regime. ζ is the distance from upper surface into layer, Δ is the boundary layer thickness = $(8M\mu)^{-1}$ ..... Fiedler and Wille (1972); ——— Kulacki and Goldstein (1972)

The Planetary Skin Model

Since all of the heat generated within the molten layer is radiated away from the top surface, the temperature in the boundary layer close to that free surface must fall to the value on the top surface to enable the thermal flux to be conducted to the surface. The general behaviour in this case will be similar to that for a Tritton-Zarraga model with slippery upper surface whose temperature varies with position on the surface. Such a temperature distribution would have to be determined rather than specified ab initio.

DISCUSSION

The convective cooling parameter M is defined by $(T^* - T_o)/(T_{max}-T_o)$ where in core catcher work T_o is the melting temperature of UO_2, T^* is the maximum temperature that would occur if only conduction were present $(= T_o + \frac{HL^2}{8k}$ for the Kulacki-Goldstein problem) and T_{max} is the maximum horizontally averaged temperature which does occur. The flux ratio μ is the ratio of heat flux through the upper surface to the total heat generated within the layer. In terms of Nusselt numbers $\mu = Nu_{up}/(Nu_{up} + Nu_{down})$. By knowing M and μ as functions of R^* we can, if the heating rate is given, place upper bounds on the depths of molten layers which can be cooled without boiling and without melting through the supporting catcher. Once the disposition of heat fluxes and the thickness of the molten layer is known, then the overall temperature structure of a layer cake composed of some or all of catcher, liner, solid radioactive UO_2, molten layer, solid radioactive layer core débris, coolant can be calculated simply using the steady state conduction equation:

$$k \frac{\partial^2 T}{\partial z^2} + H = 0$$

with appropriate interface conditions. For example for 30 MW/m^3 residual power rating, a layer of UO_2 of thickness $\simeq$ 4.5 cm can be cooled by coolant at 600^0 C above it while sitting on a catcher whose temperature does not exceed 800^0 C, provided the catcher is only $\simeq$ 1 cm thick. The layer of UO_2 consists of three almost equal sublayers: solid crust above and below the molten layer.

The algorithm for calculating the maximum thickness of molten material which does not exceed some specified temperature (for example, the boiling temperature), can be expressed as follows: When all properties of the fluid which go into the Rayleigh number for internal heat sources are known (viz α, g, H, ν, K, k) then a critical layer depth L_o can be defined by:

$$L_o = \left(Ra_{crit} \cdot \frac{\nu K k}{\alpha g H} \right)^{1/5}$$

where Ra_{crit} is the appropriate critical Rayleigh number for the boundary conditions. Then the relative Rayleigh number $R^* = (L/L_o)^5$. Eliminating L from M and R^* , we obtain

$$M = \frac{H L_o^{\,2}}{8k(T_{max} - T_o)} \cdot R^{*\,2/5} \equiv c_1 R^{*2/5}$$

If T_o is the melting temperature of UO_2 and T_{max} is the boiling temperature then the coefficient c_1 is known. For the maximum non-boiling layer depth the corresponding M and R^* are given by the intersection of the curve $M = c_1 R^{*\,2/5}$ with the empirical $M = f(R^*)$ found from laboratory and numerical experiments. The maximum molten layer depth is than $L_{max} = L_o R^{*\,1/5}_{max}$. This algorithm holds for all four model problems considered.

The effect of having no upper solid crust and radiation into space is to allow the mean temperature of the upper surface to be elevated above the melting point. The free surface enables more liquid to be brought closer to the surface. The heat flux curves for free and rigid surfaces are similar when normalized for R^* so that L_{max} may be $2^{1/5}$ smaller for a free upper surface since the appropriate Ra_{crit} is smaller. Moreover the solid upper crustal radioactive UO_2 is now absent; thus it seems likely that a smaller depth of core débris can be cooled radiatively than when coolant is present.

The core débris will not be composed purely of fuel. The cans, and their supports, and the diagrid material will provide much ferrous material. The boiling point of steel is comparable with the melting point of UO_2 , while the density of steel is 20% less than that of UO_2 . The steel débris will thus occur as inclusions (solid or liquid) whithin solid UO_2 , as a sort of blanket between solid crustal UO_2 and the coolant, and as pockets of vapour or buoyant liquid at the top of the molten layer below any solid crust. Since the thermal conductivity of steel is much larger than that of UO_2 , the steel will provide low thermal resistance, and will mainly have the effect of thickening the overall 'lump'. With a 50:50 division between heat producing UO_2 and the rest of the débris, even with internal convection within the molten layer, a consolidated layer of UO_2/steel core debris greater than $\simeq$ 10 cm will not sit passively on the core catcher.

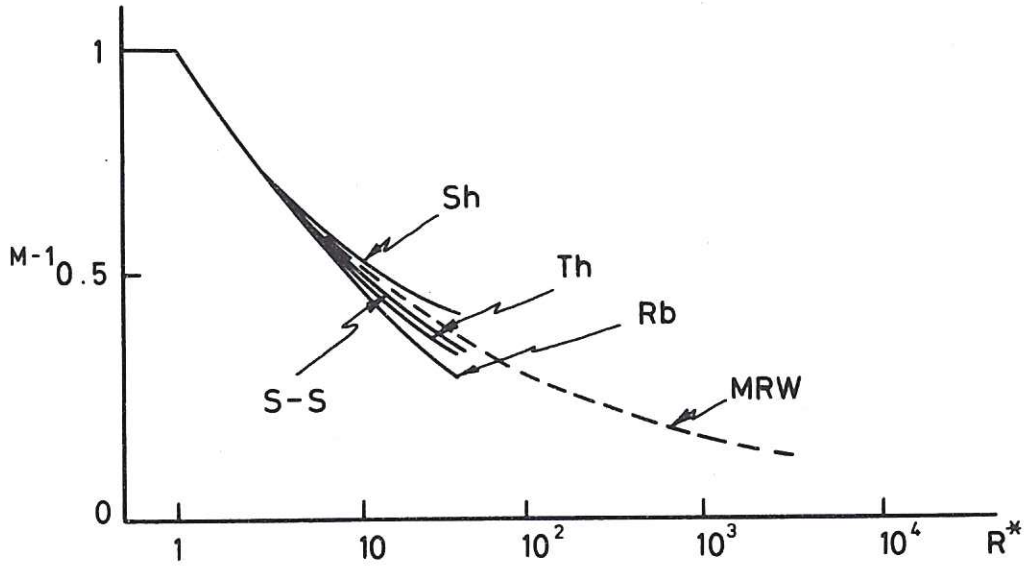

Figure 8. The convective cooling parameter $M=(T^*-T_o)/(T_{max}-T_o)$ as a function of R^* for model II. Sh≡ Shape assumption form; Th≡ Thirlby (1970); Rb≡ Roberts (1967); S-S≡ Schwiderski and Schwab (1971); MRW ≡ McKenzie, Roberts, Weiss (1974).

These models have been extreme cases in the sense that thermal resistance outside the molten layer is taken to be total, or zero. The effect of finite resistance on the critical Rayleigh number is to reduce it by factors of the order of the two compared with zero thermal resistance cases, and to produce narrower cells (Hurle et al (1967), Kulacki (1971)). It seems likely that changes in Ra_{crit} will have little effect on the dependence of M and μ on R^*. The narrower cells could enhance the fraction of heat transported upwards but this may simply counteract the effect of the finite thermal resistance.

In catchers using liners with high thermal resistance, hot spots might develop within the fluid close to the lower molten surface and this could lead to scallopping of the horizontal surface. This is a self limiting process, however, for the liner would be thinned locally so that its thermal resistance would be reduced, and the flux would reach a steady rate.

The results of this analysis give smaller maximum layer depths than one might normally expect to occur, because lumps can be cooled from their sides as

well as from the top and bottom. However in reactor safety work one should use as reference models the least favourable cases which have a reasonable probability of occurring.

An obvious extension of this work involves boiling heat transfer. For internal catchers the boiling heat transfer will subject any solid crust of UO_2 to turbulent pressure pulses, possibly breaking it and dispersing some of the core débris. The enhanced upward heat transfer makes the catcher less likely to burn through, but makes the arrival of core débris at the reactor bottom more likely. If the reactor bottom is already being used as the catcher, then the production of débris spray makes little difference if the coolant is present, whereas the enhanced heat transfer is beneficial.

In a pit-type catcher without coolant above, the boiling core débris will relieve some of the thermal stress on the lower part of the crucible. Provided the main part of the reactor is shielded from flying débris, then boiling heat transfer is desirable.

In summary, the maximum depth of débris which can be cooled when convection within the débris is allowed for (but not boiling) is probably not more than about a factor of two greater than the maximum depth when only conduction is used.

APPENDIX I

In order to be able to compare problems with different boundary conditions it is convenient to normalize the appropriate Rayleigh number relative to the critical Rayleigh number. The two idealized cases of most relevance are (1) the layer with fixed temperature on its upper surface and no thermal flux through the lower surface (the Tritton-Zarraga Model); and (2) the layer with the same constant temperature at the top and bottom surfaces (the Kulacki-Goldstein Model). As the definition for the Rayleigh number for volumetrically heated layers has a variety of different numerical factors introduced by different authors (a list is to be found in an appendix of (Peckover and Hutchinson 1973b)), two different Rayleigh numbers are quoted here:

$$\text{(i)} \quad Ra_H \equiv \frac{\alpha g H L^5}{\nu K k}$$

where α is the coefficient of thermal expansion, g is the acceleration due to gravity, L is the total depth of the layer of liquid, H is the volumetric heating rate, ν is the kinemetic viscosity, K is the thermal diffusivity, and k is the thermal conductivity.

$$\text{(ii)} \quad Ra_I \equiv \frac{\alpha g T^* L^3}{\nu K}$$

where T^* is the maximum temperature difference in the layer. Note that if $\Gamma \equiv Ra_H/Ra_I$ then $\Gamma = 8$ for case 2 and $\Gamma = 2$ for case 1. The mean temperature gradient in the unstable part of the fluid provides a convenient physical measure and the values for Bénard convection are given for comparison in Table 2. The temperature gradient at the upper surface which is a measure of upward going thermal flux is also given, as a multiple of β_o, the critical temperature gradient of the classical Rayleigh-Bénard problem.

APPENDIX II

For the Kulacki-Goldstein problem, the Jahn-Reineke data gives $M = R^{*0.18}$ (from Figure 5). Hence

$$T_{max} - T_o = \frac{1}{8}\left(Ra_H^{crit}\,\frac{\nu K}{\alpha g}\right)^{0.62}\left(\frac{H}{k}\right)^{0.38} L_{max}^{-1.1}$$

For the Tritton-Zarraga problem, $M = R^{*0.24}$ is a good approximation to the empirical function $M = f(R^*)$ from figure 8. It follows that

$$T_{max} - T_o = \frac{1}{2}\left(Ra_H^{crit}\,\frac{\nu K}{\alpha g}\right)^{0.56}\left(\frac{H}{k}\right)^{0.44} L_{max}^{-0.8}$$

TABLE 2.

Critical Rayleigh numbers for the onset of convection (see Figure 9 for the precise configuration). A 'free' boundary means here, one with no tangential stresses; a 'rigid' boundary means one where velocity $\underline{v} = 0$.

(a) Bénard Convection

	Ra^{crit}	Critical temperature gradient β
Free/Free	657.5 $(\frac{27}{4}\pi^4)$	β_o
Free/Rigid	1100.65	$\sim \frac{5}{3}\beta_o$
Rigid/Rigid	1707.762	$2.6\ \beta_o$

TABLE 2. (Continued)

(b) Convection with internal heat sources $\frac{\partial T}{\partial z} = 0$ on $z = 0$; T_L on $z = L$; $T^* \equiv T_{max} - T_L$

bottom/top	Ra_H^{crit}	Ra_I^{crit}	mean temperature gradient T^*/L	surface temperature gradient $\frac{\partial \Gamma}{\partial z}\Big\|_{z=L}$
Free/Free	867.8	433.9	$0.66\beta_o$	$1.32\beta_o$
Rigid/Free	1612.6	806.3	$1.23\beta_o$	$2.46\beta_o$
Free/Rigid	1650.6	825.3	$1.25\beta_o$	$2.50\beta_o$
Rigid/Rigid	2772	1336	$2.10\beta_o$	$4.20\beta_o$

(c) Convection with internal heat sources $T = T_L$ on $z = 0$ and $z = L$; $T^* = T_{max} - T_L$

bottom/top	Ra_H^{crit}	Ra_I^{crit}	mean unstable temperature gradient $T^*/(\frac{1}{2}L)$	surface gradient $\frac{\partial \Gamma}{\partial z}\Big\|_{z=L}$
Free/Free	16,977	2122.10	$6.4\beta_o$	$12.8\beta_o$
Rigid/Free	16,655	2081.90	$6.3\beta_o$	$12.6\beta_o$
Free/Rigid	37,950	4743.70	$14.4\beta_o$	$28.8\beta_o$
Rigid/Rigid	37,325	4665.60	$14.1\beta_o$	$28.2\beta_o$

(after Kulacki (1971), Sparrow et al (1963)).

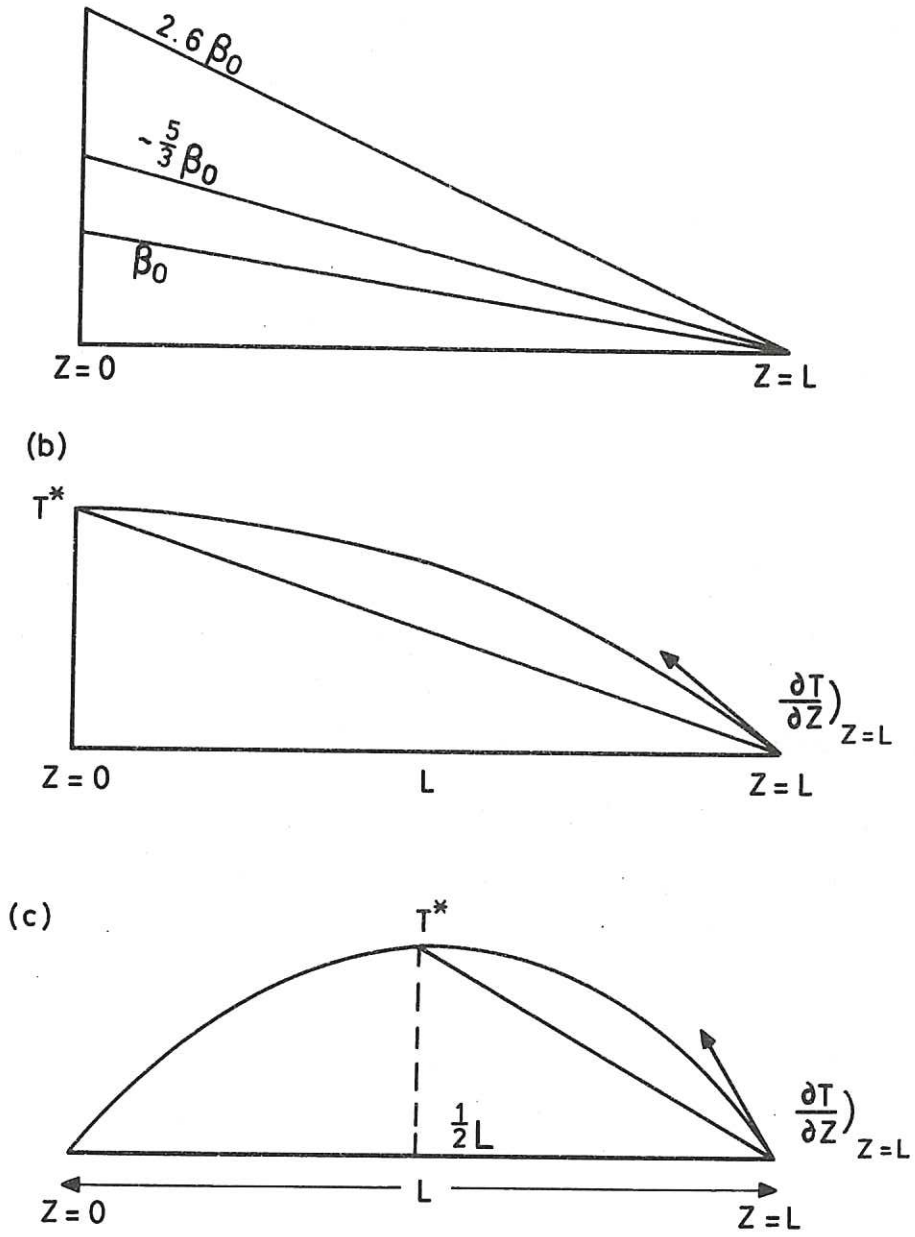

Figure 9. (a) Bénard convection (β_0 is the applied gradient necessary to produce thermal instability in a layer with free upper and lower boundaries - the classical Rayleigh-Bénard problem)

(b) convection driven by internal heat sources when the lower surface is a thermal insulator and the upper surface is at fixed temperature (Tritton-Zarraga problem)

(c) convection driven by internal heat sources when both upper and lower surfaces are at the same fixed temperature (Kulacki-Goldstein problem)

ACKNOWLEDGEMENTS

I am grateful to Drs Jahn and Reineke and to Professor Catton for preprints of their papers and to Dr Schwiderski for additional data. This work was performed under the aegis of the Safety and Reliability Directorate of the UKAEA.

REFERENCES

Baker L, and Gabor J (1972) - "Internal Heat Generation in Particulate Beds" ANL-RDP-5.

Board S J, Farmer C L, and Poole D H (1972) - CEGB Report RD/B/N2423.

Brindley J (1967) - J.Inst. Maths Applics. 3, 313-343.

Buchanan D J (1973) - UKAEA Culham preprint P-361.

Buchanan D J and Dullforce T A (1973) - Nature 245, 32.

Catton I, and Suo-Anttila (1973) - Heat Transfer from a volumetrically heated horizontal layer (private communication).

Chasanov M G, Leibowitz L and Gabelnick S D (1974), J.Nucl. Materials 49, 129.

Epstein M (1972) - ANL-RDP-7 - July - Argonne National Laboratory.

Ergen W K et al (1967) - "Emergency Core Cooling - Report of US Advisory Task Force on Power Reactor Emergency Cooling".

Hurle D T J, Jakeman E, Pike E R (1966) Proc.Roy.Soc. A 296, 469.

Jahn M, and Reineke H H (1973) - Free Convection Heat Transfer with Internal Heat Sources: Calculations and Measurements (private communication).

Kulacki F A (1971) - Ph.D. Thesis - University of Minnesota.

Kulacki F A and Goldstein R S (1972) J.Fluid Mech. 55, 271.

McKenzie D P, Roberts J M and Weiss N O (1974)- J.Fluid Mech. 62, 465.

Moore D R and Weiss N O (1973) - J.Fluid Mech. 58, 289.

Peckover R S (1973) - in Proc.Conference on Fast Reactor Safety, Karlsruhe, Oct 1973.

Peckover R S and Hutchinson I H (1973a) - UKAEA Culham preprint CLM-P355 to be published.

Peckover R S and Hutchinson I H (1973b) - UKAEA Culham Report CLM-R123.

Peckover R S and Hutchinson I H (1974) - In preparation.

Roberts P H (1967) - J.Fluid Mech. 30, 33-49.

Schwiderski E W (1972) - Phys.Fluids 15, 1189.

Schwiderski E W and Schwab H J A (1971), J.Fluid Mech. 48, 703.

Sparrow E M, Goldstein R J and Jonsson V K (1964) - J.Fluid Mech. 18, 513.

Teague H J (1965) - private communication.

Thirlby R (1970) - J.Fluid Mech. 44, 673.

Tritton D J and Zarraga M N (1967) - J.Fluid Mech. 30, 21.

Tsai H C and Olander D R (1972) - Trans.ANS 15, 211.

Whitehead J A and Chen M M (1970) - J.Fluid Mech. 40, 549.